

Article

Efficiency of Iron-Based Oxy-Hydroxides in Removing Antimony from Groundwater to Levels below the Drinking Water Regulation Limits

Konstantinos Simeonidis ¹, Vasiliki Papadopoulou ¹, Sofia Tresintsi ¹, Evgenios Kokkinos ¹, Ioannis A. Katsoyiannis ², Anastasios I. Zouboulis ² and Manassis Mitrakas ^{1,*}

¹ Department of Chemical Engineering, Aristotle University of Thessaloniki, 54124 Thessaloniki, Greece; ksime@physics.auth.gr (K.S.); papadovm8@gmail.com (V.P.); tresintsi@yahoo.gr (S.T.); kokkinosevgenios@yahoo.gr (E.K.)

² Department of Chemistry, Aristotle University of Thessaloniki, 54124 Thessaloniki, Greece; katsogia@chem.auth.gr (I.A.K.); zoubouli@chem.auth.gr (A.I.Z.)

* Correspondence: manassis@eng.auth.gr; Tel.: +30-231-099-6248

Academic Editor: Marc A. Rosen

Received: 22 November 2016; Accepted: 5 February 2017; Published: 10 February 2017

Abstract: This study evaluates the efficiency of iron-based oxy-hydroxides to remove antimony from groundwater to meet the requirements of drinking water regulations. Results obtained by batch adsorption experiments indicated that the qualified iron oxy-hydroxide (FeOOH), synthesized at pH 4 for maintaining a high positive charge density (2.5 mmol OH⁻/g) achieved a residual concentration of Sb(III) below the EU drinking water regulation limit of 5 µg/L by providing an adsorption capacity of 3.1 mg/g. This is more than twice greater compared either to similar commercial FeOOHs (GFH, Bayoxide) or to tetravalent manganese ferrihydroxide (Fe-MnOOH) adsorbents. In contrast, all tested adsorbents failed to achieve a residual concentration below 5 µg/L for Sb(V). The higher efficiency of the qualified FeOOH was confirmed by rapid small-scale column tests, since an adsorption capacity of 3 mg Sb(III)/g was determined at a breakthrough concentration of 5 µg/L. However, it completely failed to achieve Sb(V) concentrations below 5 µg/L even at the beginning of the column experiments. The results of leaching tests classified the spent qualified FeOOH to inert wastes. Considering the rapid kinetics of this process (i.e., 85% of total removal was performed within 10 min), the developed qualified adsorbent may be promoted as a prospective material for point-of-use Sb(III) removal from water in vulnerable communities, since the adsorbent's cost was estimated to be close to 30 ± 3.4 €/10³ m³ for every 10 µg Sb(III)/L removed.

Keywords: antimony; drinking water; adsorption; iron oxy-hydroxides; column tests; surface charge

1. Introduction

Antimony is classified as a toxic compound and as a high priority pollutant, especially for water supplies used for drinking purposes [1]. Particularly, international organizations (US EPA, EU) have established a very low maximum permissible contaminant level (6 and 5 µg/L, respectively) for Sb species regarding the consumption of safe drinking water [2,3]. Nevertheless, particular attention has not been dedicated to the understanding of Sb aqueous chemistry, as well as to the development of respective methods for its efficient removal to levels below the regulation limits. This can be attributed to the lower frequency of the presence of Sb in aquatic systems, which is a consequence of its limited solubility, when compared to aquatic species of other elements of the same group in the Periodic Table, such as arsenic and phosphorus [4]. Still, high concentrations of Sb were reported in water sources near hot springs, in areas with specific industrial activities such as the production of flame retardants,

batteries, chemicals, ceramics, etc., as well as in certain mining fields. In the last case, the presence of antimony is usually combined with high arsenic concentrations, mainly originating from sulfide ores [5].

In natural waters, Sb can be found in two oxidation states, i.e., as Sb(III) and Sb(V), depending on the respective redox potential of the aquatic reservoir. Under oxic conditions, Sb(V) oxyanions are the dominant forms, while the percentage of trivalent species, considered to be more toxic, becomes significant only in less oxygenated systems. The speciation of Sb(V) is determined by its coordination with oxygen atoms which is rather different from the corresponding As(V) and P(V) oxyanions. More specifically, due to its larger ionic radius and lower charge density, Sb(V) is coordinated in octahedral geometry, unlike As(V) and P(V) which favor a tetrahedral formation. Accordingly, Sb(OH)_6^- is the dominant species of Sb(V) in the common pH range of natural waters. On the other side, neutral Sb(OH)_3 species appear as the hydrolyzed forms of Sb(III).

A variety of methods have been proposed for the removal of Sb from water, with most of them being adapted by similar approaches as applied in the case of arsenic removal. In summary, coagulation, adsorption, oxidation, ion-exchange, membrane separation and bioremediation techniques are commonly discussed in the respective literature studies [6,7]. Coagulation and co-precipitation methods usually incorporate the use of low-cost ferric or aluminum salts to successively capture both Sb(III) and Sb(V) species [8–11]. Relevant studies indicate that the removal of Sb(III) is more favorable than that of Sb(V), due to the increasing mobility of pentavalent species at pH values above 5 and the strong competition for adsorbing sites of specific co-existing anions, such as phosphate, silicate, and bicarbonate, commonly found in natural waters. Among the available treatment processes, the application of adsorbents in the column bed filter configuration is considered as a more advantageous setup due to its simplicity and almost unattended operation. Iron-based oxy-hydroxides (FeOOHs) are the main class of adsorbents studied so far for Sb uptake, while other solid phases or inorganic composites, including zero valent iron [12], graphene oxide [13,14], activated alumina [15], aerobic bio-granules [16], hydroxyapatite [4] and zeolites [17], were also reported as alternative active adsorption materials.

In general, the adsorption behavior of antimony onto FeOOHs is determined mainly by its speciation (as Sb(III) and/or Sb(V)), its affinity with the different kinds of adsorbents, the pH of adsorption, interferences by other co-existing competing ions, and by secondary desorption processes [18–21]. Both Sb species form inner-sphere complexes when adsorbed on a FeOOH surface [22]. However, the literature results suggest that the adsorption of Sb(III) is almost independent of the applied pH value, whereas the adsorption capacity for Sb(V) significantly drops as the pH increases within the pH range of natural waters (6–8) and decreases further in the presence of certain competing anions such as phosphates.

Another important observation is that the surface of amorphous FeOOH may catalyze the oxidation of initially adsorbed Sb(III), leading to the partial desorption of Sb(V) back into the treated water [23,24]. This mechanism becomes more intense when applying iron-manganese oxy-hydroxides (Fe-MnOOH), due to the rapid oxidation of Sb(III) and the subsequent release of formed Sb(V) [25,26]. Although this strategy promotes the advantage of converting antimony to the less toxic Sb(V) species, the result of this reaction is of doubtful use, since efficient adsorption results for Sb(V) can be provided only for acidic pH values (i.e., below 5); therefore, it is not particularly useful for drinking water applications.

From the practical point of view, the treatment/removal of antimony from water by using adsorbents has to be approached in a different way than in the system of As(III)/As(V). Many studies indicate that commercial sorbent materials based on FeOOH developed for arsenic removal fail to be efficient for the removal of antimony. Particularly, granular ferric hydroxide (GFH), CFH12 or Bayoxide E33 have been tested in several studies, indicating a weak performance for antimony removal, i.e., one to two orders of magnitude below the corresponding values for arsenic, since the adsorption capacity at the residual concentration of 5 $\mu\text{g/L}$ ranged between 0.03 and 0.65 mg Sb/g [27–30].

The aim of this work is to determine the major parameters featuring an effective iron oxy-hydroxide adsorbent material that can enable a high potential for antimony uptake, i.e., able to provide a residual Sb concentration below the respective drinking water regulation, and to suggest a relatively simple preparation method that can create such a customized material. To the best of our knowledge, the application of this kind of FeOOH has not been previously reported and comprises a fully new approach in antimony removal options, which leaves the field for further improvements open. In this regard, a series of FeOOH was prepared by the precipitation of iron salts under different pH and redox potential values. The adsorption capacity of these adsorbents for Sb(III) and Sb(V) species was evaluated in comparison to commercial FeOOH- and Fe-MnOOH-based products, already used for arsenic treatment, by applying batch and column experimental protocols.

2. Materials and Methods

2.1. Adsorbents

In order to establish the correlation of structural and surface properties of FeOOH with their efficiency to capture/remove antimony, a series of samples were synthesized by oxidation-hydrolysis of $\text{FeSO}_4 \cdot \text{H}_2\text{O}$ under high redox potential and various pH values, using a laboratory two-stage continuous flow reactor [31]. The reaction setup was pumped with a 40 g/L $\text{FeSO}_4 \cdot \text{H}_2\text{O}$ solution at a 10 L/h rate, whereas redox potential and pH were regulated by the addition of drops of H_2O_2 (50% w/w) and NaOH (30% w/w), respectively. Particularly, in each synthesis, the pH was set at a constant value (4, 7, 9) and for this condition the redox potential was controlled to the corresponding maximum point, before oxygen bubbles appear, i.e., from +410 to +170 mV for the specific pH range. Formed solids were collected from the outflow of the system and thickened using an Imhoff tank. The obtained sludge was washed, centrifuged and dried for 4 h at 110 °C. The material was ground either as fine powder (with size less than 63 μm) for the batch adsorption experiments, or as granules (with size 0.25–0.50 mm) for the column tests. The specific surface area of the samples was determined by the volumetric method (BET) in the range 120–150 m^2/g . The production cost of such process scaled up to industrial-operation terms is estimated to be around 2 €/kg split to 0.9 €/kg for reagents, 0.2 €/kg for energy, 0.4 for labor and 0.5 €/kg for other (maintenance, packaging, depreciation, etc.) costs. For comparison reasons, the commercially available FeOOH and Fe-MnOOH products approved for arsenic treatment, such as GFH (237 m^2/g), AquAsZero (190 m^2/g), Bayoxide (135 m^2/g) namely consisting of akagaenite, tetravalent manganese ferrihydroxide and goethite, respectively, were also examined in this study.

2.2. Batch Experiments

Stock solutions of Sb(III) or Sb(V) (100 mg/L) were prepared from reagent grade Sb_2O_3 and $\text{K}[\text{Sb}(\text{OH})_6]$, respectively. Working standards were freshly prepared by proper dilution of the stock solutions in a test water matrix, containing the interfering ions of a typical natural water. The natural-like water was prepared according to National Sanitation Foundation (NSF) standard, containing 252 mg NaHCO_3 , 12.14 mg NaNO_3 , 0.178 mg $\text{NaH}_2\text{PO}_4 \cdot \text{H}_2\text{O}$, 2.21 mg NaF, 70.6 mg $\text{NaSiO}_3 \cdot 5\text{H}_2\text{O}$, 147 mg $\text{CaCl}_2 \cdot 2\text{H}_2\text{O}$ and 128.3 mg $\text{MgSO}_4 \cdot 7\text{H}_2\text{O}$, diluted in 1 L of distilled water. Prior to adsorption experiments, pH was adjusted to the target value, by adding either NaOH or HCl of 0.1 or 0.01 N. Adsorption batch experiments were carried out by placing 5–25 mg of adsorbents' fine powder, with size less than 63 μm , in 300 mL conical flasks and shaking with 200 mL of aqueous Sb(III) or Sb(V) solutions for 24 h at 20 °C. Initial antimony concentrations ranged between 100 and 5000 $\mu\text{g}/\text{L}$ to provide equilibrium concentrations between 2 and 1000 $\mu\text{g}/\text{L}$. Initial pH values were adjusted at 6, 7 and 8 and adsorption isotherms were recorded at each equilibrium pH. At the end of each experiment, the suspensions were filtered through a 0.45 μm pore-size membrane filter. The collected samples (100 mL) were first acidified by adding 1 mL of 8 N HNO_3 and then antimony species were stabilized in the Sb(V) form with the addition of 0.2 mL of 0.1 N KMnO_4 . Initial and residual antimony

concentrations were determined by Graphite Furnace Atomic Absorption Spectrophotometry, using a Perkin-Elmer AAnalyst 800 instrument, with a calibration curve of Sb(V) standards. The detection limit of the method, which was calculated from 7 replicates of 2–10 µg Sb/L, was estimated to be 1.5 µg/L.

2.3. Kinetics

The evolution of antimony concentration with contact time (0–24 h) was monitored during batch adsorption experiments, by introducing 20 mg of adsorbent dispersed in 200 mL of Sb(III) solution in NSF water matrix with initial concentration 500 µg/L at pH 7 and 20 °C. Sampling was performed with higher frequency during initial treatment times, whereas it was performed at extended time intervals, when equilibrium was approached.

2.4. Column Tests

Rapid small-scale column tests (RSSCT) were performed to evaluate the efficiency of tested adsorbents in a full-scale system, by designing the experiments in such a way that would simulate a full-scale adsorption column with an Empty Bed Contact Time (EBCT) of 5 min. This was achieved by operating a small-scale laboratory experiment with an EBCT 3 min, using a Reynolds-Schmidt numbers product of around 2000, and an hydraulic loading q of 0.5 L/h. Granules of adsorbents with size 0.25–0.50 mm were introduced in laboratory glass columns (of 1.1 cm diameter and 40 cm height), equipped with PTFE valves and a glass frit to hold the material. Columns were filled at a height of 26 cm by granules of the qualified FeOOH adsorbent ($m_{ads} = 15$ g) and AquAsZero ($m_{ads} = 12$ g). The system was fed either by Sb(III) or Sb(V) solution ($C_0 = 100$ µg/L) in NSF water matrix pumped from the top of the column. The equilibrium pH was adjusted to 7 ± 0.1 . Water samples were periodically collected from the effluent and analyzed for the residual antimony concentration (C_e). The adsorption capacity Q (mg·Sb/g adsorbent) at each time t was determined by the implementation of Equation (1):

$$Q = \sum_{t=0}^t (C_0 - C_e) \cdot q \cdot dt / m_{ads} \quad (1)$$

2.5. Leaching Behavior

Antimony desorption tests were performed by using the spent adsorbents from RSSCT experiments to check their compliance with the regulations for environmentally safe disposal. A given mass of the solid-loaded with Sb sample was placed in a container with a specific volume of a leaching solution, according to standard leaching test EN 12457 [32].

3. Results

3.1. Adsorption Evaluation

The optimum preparation conditions for the synthesized FeOOHs were determined according to their efficiency to remove antimony species from water, by evaluating the corresponding adsorption isotherms in the pH range commonly encountered in drinking water. Figure 1 presents the results for the representative adsorbents synthesized at pH values of 4, 7 and 9, which were tested in batch adsorption experiments for Sb(III) and Sb(V) removal from NSF water. The isotherms were extended to higher Sb concentrations than those usually encountered in natural water to better clarify the existence of any trend and to obtain a more accurate fitting of the results. It is demonstrated that all examined materials appear to be potentially efficient for Sb(III) uptake, with the maximum adsorption capacity achieved by the FeOOH synthesized at pH 4, which in turn was qualified as the optimum adsorbent. By the fitting of the Sb(III) adsorption data by a Freundlich-type curve, an adsorption capacity at the residual concentration of 5 µg/L equal to 3.1 mg/g was estimated for the qualified adsorbent, which is abbreviated as Q_5 henceforth. However, the Q_5 value was decreased close to 2 mg/g when the synthesis procedure took place at neutral or alkaline pH values. On the other hand, the tested

adsorbents were not proved able to achieve final Sb(V) concentrations below the regulation limit of 5 µg/L, indicating very low capacities in the studied residual concentration range (Figure 1b).

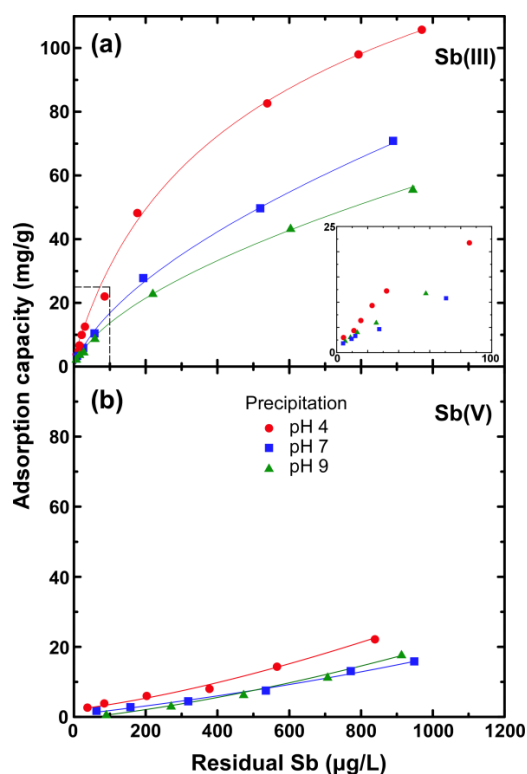


Figure 1. Antimony adsorption isotherms for synthesized FeOOH samples prepared by precipitation at pH values 4, 7 and 9; uptake of (a) Sb(III), and (b) Sb(V), dissolved in NSF water at pH 7. Inset: magnification of the isotherm in the concentration range 0–100 µg/L.

The efficiency of the qualified FeOOH for Sb(III) adsorption was relatively stable in the water pH range of 6–7, where the dominant antimony form is Sb(OH)₃ (Figure 2). However, the adsorption capacity slightly decreased when the adsorption took place either under more acidic (pH 5) or more alkaline conditions (pH 8). In addition, the qualified FeOOH was found to be more efficient for the removal of Sb(III), when compared to certain commercially available arsenic adsorbents.

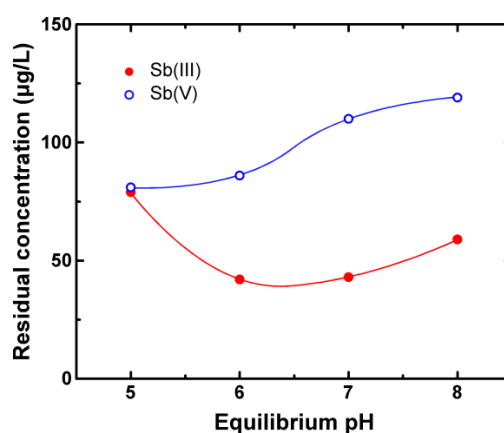


Figure 2. Influence of water pH on Sb species adsorption efficiency of qualified FeOOH. Initial concentrations: 1000 µg Sb(III)/L, 250 µg Sb(V)/L, Adsorbent 50 mg/L, NSF water matrix, 20 °C. Estimated loadings: 18.4–19.1 mg/g for Sb(III) and 2.6–3.4 mg/g for Sb(V).

GFH and Bayoxide provided lower Q_5 values of 1.4 mg/g and 0.6 mg/g, respectively, while AquAsZero was unable to reduce the residual Sb(III) below the limit value of 5 $\mu\text{g/L}$ (Figure 3). Similarly, the commercial FeOOH adsorbents failed to meet the drinking water regulation limit for Sb(V) (data not shown).

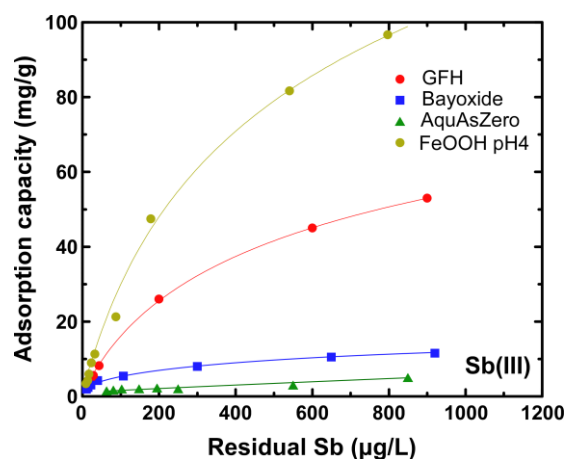


Figure 3. Sb(III) adsorption isotherms for GFH, Bayoxide and AquAsZero, which are commercially available adsorbents, in comparison to that of FeOOH prepared at pH 4. Experiments were conducted in NSF water matrix at pH 7.

3.2. Kinetics

The evolution of the residual Sb(III) concentration by increasing the contact time during the batch experiments indicated a very rapid adsorption process, as 85% removal was observed within the first 10 min of contact time, while 96% of the equilibrium concentration was reached after the first hour. Figure 4 shows the kinetic data obtained for the FeOOH samples prepared at pH values of 4 (qualified FeOOH) and 7. These experimental points were best fitted by a pseudo-second-order equation:

$$\frac{t}{q_t} = \frac{1}{kq_e^2} + \frac{t}{q_e} \quad (2)$$

where t is the contact time (min), q_t the adsorption capacity at this time (mg/g), q_e the maximum capacity at equilibrium and k the corresponding adsorption constant (g/mg·min). The fitting parameters q_e and k were estimated to be 4.043 mg/g and 1.050 g/(mg·min), respectively, for the adsorbent prepared at pH 4, while the corresponding values for the adsorbent prepared at pH 7 were 3.326 mg/g and 0.823 g/(mg·min). Since the FeOOH samples were porous particles that were vigorously agitated during the adsorption period, it is reasonable to assume that the rate was not limited by mass transfer from the bulk liquid to the external surface of particles. The fact that the inclined lines (inset of Figure 4) do not pass through the origin verifies this assumption, indicating simultaneously that the limiting rate step of adsorption is attributed to the intraparticle diffusion effect and the plateau to the equilibrium [33].

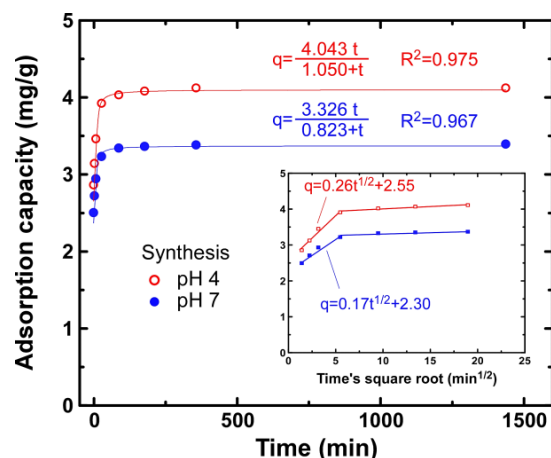


Figure 4. Kinetic data for Sb(III) adsorption fitted by a pseudo-second-order function for the FeOOH samples synthesized at pH 4 (qualified FeOOH) and 7, in NSF water adjusted at pH 7.

3.3. Column Experiments

Figure 5 summarizes the breakthrough curves for both Sb(III) and Sb(V) uptake by the qualified FeOOH, as well as by the commercial AquAsZero. The commercial FeOOH products GFH and Bayoxide were not studied further here due to the previous publications of relevant data from large-scale column operations [30,34]. The results show that the efficiency of the qualified FeOOH, prepared in this study, at the breakthrough concentration of 5 $\mu\text{g}/\text{L}$, was approaching the Q_5 value of 3 mg/g for Sb(III) removal, which is close to that defined by the batch adsorption experiments (Section 3.1). This Q_5 value corresponds to 19.2×10^3 bed volumes. On the contrary, AquAsZero provided a Q_5 value of only 0.2 mg/g for Sb(III) due to the oxidation of the latter to Sb(V). It should be clarified that AquAsZero was incorporated in this study just to illustrate the negative effect of oxidation in antimony removal. In any case, however, both adsorbents completely failed to capture the Sb(V) species even during the initial times of the column experiments, thus confirming the results of our batch experiments.

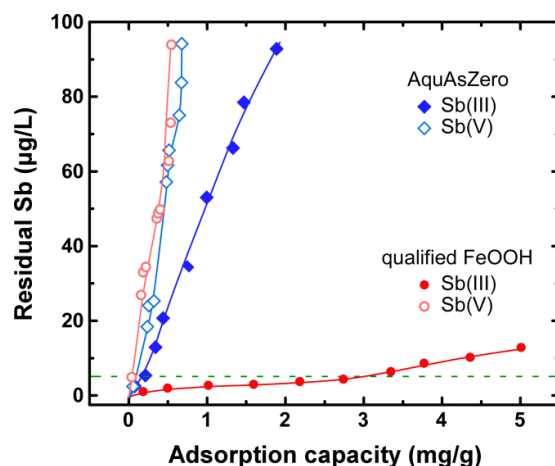


Figure 5. Breakthrough curves of granular qualified FeOOH and AquAsZero for Sb(III) and Sb(V) removal during RSSCT experiments. Initial concentration 100 $\mu\text{g}/\text{L}$ in NSF water, adjusted at pH 7.

3.4. Leaching Tests

The spent adsorbents from the RSSCT experiments were subjected to leaching tests according to the EN 12457 procedure. The leaching results of the spent adsorbents loaded by Sb(III) indicated

that the qualified FeOOH should be treated as inert waste, while AquAsZero should be treated as non-hazardous waste (Table 1). In contrast, both adsorbents should be characterized as non-hazardous wastes after Sb(V) uptake.

Table 1. Leaching characteristics of spent adsorbents tested in RSSCT experiments.

Spent Adsorbent	Adsorption Load (mg·Sb/g)	EN12457-01 (mg/kg) ¹
<i>Sb(III)</i>		
Qualified FeOOH	5.1	0.05
AquAsZero	3.4	0.22
<i>Sb(V)</i>		
Qualified FeOOH	0.30	0.55
AquAsZero	0.35	0.68

¹ Limit for inert wastes 0.06 mg Sb/kg and limit for non-hazardous wastes 0.7 mg Sb/kg.

4. Discussion

An overview of the examined materials, regarding their adsorption capacity for Sb(III) as derived by batch experiments, is presented in Figure 6. The Q_5 values of synthesized FeOOHs were found to be at least 35% higher than the best commercially available adsorbent (GFH), while the capacity for the qualified FeOOH synthesized under acidic conditions (pH 4) was almost double. The direct comparison of the Q_5 values determined in this study with the relevant Sb adsorbents' efficiencies reported in literature was not possible because most of them focused on the maximum adsorption capacity, which is obtained at residual concentrations far higher than the drinking water regulation limit of 5 $\mu\text{g/L}$. With respect to the synthesis conditions, the optimization of the adsorption behavior was observed when FeOOH adsorbent presents high surface charge density. Specifically, a surface charge density of 2.5 mmol OH^-/g was determined for the qualified FeOOH, while the corresponding surface charge densities for the samples synthesized at pH values of 7 and 9 were 0.8 and 0.5 mmol OH^-/g , respectively [31].

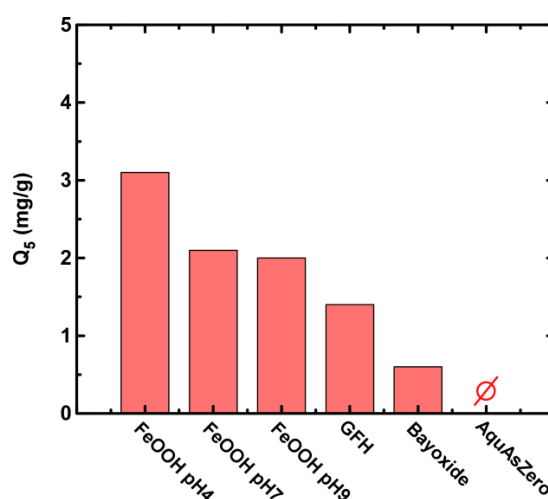


Figure 6. Q_5 values for the synthesized FeOOHs at pH 4, 7 and 9 in comparison to commercial adsorbents at NSF water adjusted to pH 7.

In addition, the pH dependence of the adsorption efficiency (Figure 2) should be correlated with the isoelectric point (IEP) of FeOOH in combination with the corresponding Sb(III) speciation (Figure 7). Particularly, at pH values below IEP (7.2), the net surface charge of FeOOH is positive, while at pH

values above IEP it becomes negatively charged [31]. Therefore, in the NSF water matrix at a pH lower than 6, a part of the Sb(III) is present in the Sb(OH)_2^+ form, which is repulsed by the positive surface of FeOOH, resulting in a lower adsorption efficiency. Similarly, at pH 8, part of the Sb(III) appears in the Sb(OH)_4^- form, which is repulsed by the negatively charged surface of FeOOH. In the case of Sb(V), Sb(OH)_6^- is the dominant form in the examined pH range (5–8). Therefore, adsorption efficiency is stable at the pH range of 5–6, where the FeOOH surface is positively charged but decreases significantly as the water pH approaches IEP and diminishes at water pH 8 where the FeOOH surface becomes negatively charged, thus repulsing antimonate oxyanions.

However, the FeOOH adsorbents were found to be effective only for Sb(III) uptake at levels able to fulfill the drinking water regulation limit of the EU. Their low affinity with Sb(V), which was observed in this study by both batch and column tests, was also verified by large-scale results. For instance, an adsorption capacity of 0.04 mg/g at a breakthrough concentration of 21 $\mu\text{g/L}$ was determined at a Melivoia (Greece) water treatment plant using Bayoxide [30], and an adsorption capacity of 0.06 mg/g was reported in a demonstration project of the US EPA using GFH [34]. Even worse, AquAsZero (Fe-MnOOH products) appear ineffective for both Sb species. The low performance of AquAsZero should be correlated with the high oxidative potential, arising with the Mn^{4+} substitution in the oxy-hydroxide structure which results in the formation of Sb(V), showing very low affinity for adsorption.

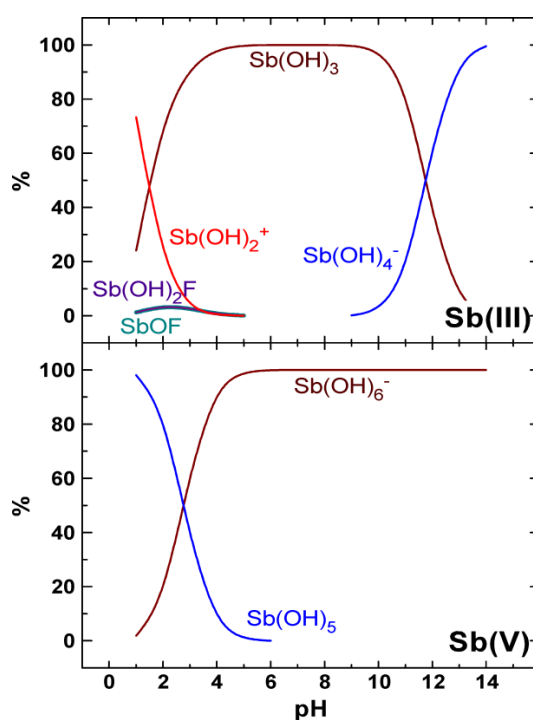


Figure 7. Speciation of Sb(III) and Sb(V) (100 $\mu\text{g/L}$) in NSF water at 20 °C. Diagrams derived by Visual MINTEQ 3.0 (<http://vminteq.lwr.kth.se>).

5. Conclusions

The developed positively charged FeOOH adsorbent may be applied as an efficient Sb(III) adsorbent, because it showed improved adsorption capacity under reliable water treatment conditions. Considering that the cost of the qualified FeOOH would be similar to that of the commercial FeOOH adsorbents (9 ± 1 €/kg), the adsorbent cost is estimated to be close to 30 ± 3.4 €/10³ m³ for every 10 μg Sb(III)/L removed. For the water treatment cost estimation, the energy cost (10 ± 1) €/10³ m³ and labor cost (10 ± 5) €/10³ m³ should be superadded, though they do not depend on the Sb(III)

concentration. Removal of Sb(V), which is the stable form in oxygenated groundwater, may therefore require a primary reduction to Sb(III) and then sorption of Sb(III) onto FeOOHs.

Acknowledgments: This work was supported by the European Commission FP7/Research for SMEs “AquAsZero”, Project No.: 232241.

Author Contributions: Anastasios I. Zouboulis and Manassis Mitrakas conceived, designed and supervised the experiments. Vasiliki Papadopoulou, Sofia Tresintsi and Evgenios Kokkinos performed the synthesis and adsorption experiments. Ioannis A. Katsoyiannis analyzed adsorption and kinetic data. Konstantinos Simeonidis and Manassis Mitrakas wrote the paper with the contribution of all co-authors.

Conflicts of Interest: The authors declare no conflict of interest.

References

1. World Health Organization. *Antimony in Drinking-Water*; Background Document for Preparation of WHO Guidelines for Drinking-Water Quality; WHO/SDE/WSH/03.04/74; World Health Organization: Geneva, Switzerland, 2003.
2. US Environmental Protection Agency. *Edition of the Drinking Water Standards and Health Advisories*; Office of Water, US Environmental Protection Agency: Washington, DC, USA, 2012.
3. European Union. *Council Directive 98/83/EC on the Quality of Water Intended for Human Consumption*; L330/32; Official Journal of the European Union: Brussels, Belgium, 1998.
4. Leyva, A.G.; Marrero, J.; Smichowski, P.; Cicerone, D. Sorption of antimony onto hydroxyapatite. *Environ. Sci. Technol.* **2001**, *35*, 3669–3675. [[CrossRef](#)] [[PubMed](#)]
5. Wilson, N.J.; Craw, D.; Hunter, K. Antimony distribution and environmental mobility at an historic antimony smelter site, New Zealand. *Environ. Pollut.* **2004**, *129*, 257–266. [[CrossRef](#)] [[PubMed](#)]
6. Ungureanu, G.; Santos, S.; Boaventura, R.; Botelho, C. Arsenic and antimony in water and wastewater: Overview of removal techniques with special reference to latest advances in adsorption. *J. Environ. Manag.* **2015**, *151*, 326–342. [[CrossRef](#)] [[PubMed](#)]
7. Mubarak, H.; Chai, L.-Y.; Mirza, N.; Yang, Z.-H.; Pervez, A.; Tariq, M.; Shaheen, S.; Mahmood, Q. Antimony (Sb)—Pollution and removal techniques—Critical assessment of technologies. *Toxicol. Environ. Chem.* **2015**, *97*, 1296–1318. [[CrossRef](#)]
8. Gannon, K.; Wilson, D.J. Removal of Antimony from Aqueous Systems. *Sep. Sci. Technol.* **1986**, *21*, 475–493. [[CrossRef](#)]
9. Wu, Z.; He, M.; Guo, X.; Zhou, R. Removal of antimony(III) and antimony(V) from drinking water by ferric chloride coagulation: Competing ion effect and the mechanism analysis. *Sep. Purif. Technol.* **2010**, *76*, 184–190. [[CrossRef](#)]
10. Guo, X.; Wu, Z.; He, M. Removal of antimony(V) and antimony(III) from drinking water by coagulation-flocculation-sedimentation (CFS). *Water Res.* **2009**, *43*, 4327–4335. [[CrossRef](#)] [[PubMed](#)]
11. Kang, M.; Kamei, T.; Magara, Y. Comparing polyaluminum chloride and ferric chloride for antimony removal. *Water Res.* **2003**, *37*, 4171–4179. [[CrossRef](#)]
12. Xu, C.; Zhang, B.; Zhu, L.; Lin, S.; Sun, X.; Jiang, Z.; Tratnyek, P.G. Sequestration of Antimonite by Zerovalent Iron: Using Weak Magnetic Field Effects to Enhance Performance and Characterize Reaction Mechanisms. *Environ. Sci. Technol.* **2016**, *50*, 1483–1491. [[CrossRef](#)] [[PubMed](#)]
13. Leng, Y.; Guo, W.; Su, S.; Yi, C.; Xing, L. Removal of antimony(III) from aqueous solution by graphene as an adsorbent. *Chem. Eng. J.* **2012**, *211–212*, 406–411. [[CrossRef](#)]
14. Dong, S.; Dou, X.; Mohan, D.; Pittman, C.U.; Luo, J. Synthesis of graphene oxide/schwertmannite nanocomposites and their application in Sb(V) adsorption from water. *Chem. Eng. J.* **2015**, *270*, 205–214. [[CrossRef](#)]
15. Xu, Y.; Ohki, A.; Maeda, S. Adsorption and removal of antimony from aqueous solution by an activated Alumina. *Toxicol. Environ. Chem.* **2001**, *80*, 133–144. [[CrossRef](#)]
16. Wang, L.; Wan, C.; Zhang, Y.; Lee, D.-J.; Liu, X.; Chen, X.; Tay, J.-H. Mechanism of enhanced Sb(V) removal from aqueous solution using chemically modified aerobic granules. *J. Hazard. Mater.* **2015**, *284*, 43–49. [[CrossRef](#)] [[PubMed](#)]
17. Wingenfelder, U.; Furrer, G.; Schulin, R. Sorption of antimonate by HDTMA-modified zeolite. *Microporous Mesoporous Mater.* **2006**, *95*, 265–271. [[CrossRef](#)]

18. He, Z.; Liu, R.; Liu, H.; Qu, J. Adsorption of Sb(III) and Sb(V) on Freshly Prepared Ferric Hydroxide (FeOxHy). *Environ. Eng. Sci.* **2015**, *32*, 95–102. [[CrossRef](#)] [[PubMed](#)]
19. Guo, X.; Wu, Z.; He, M.; Meng, X.; Jin, X.; Qiu, N.; Zhang, J. Adsorption of antimony onto iron oxy-hydroxides: Adsorption behavior and surface structure. *J. Hazard. Mater.* **2014**, *276*, 339–345. [[CrossRef](#)] [[PubMed](#)]
20. Vithanage, M.; Rajapaksha, A.U.; Dou, X.; Bolan, N.S.; Yang, J.E.; Ok, Y.S. Surface complexation modelling and spectroscopic evidence of antimony adsorption on iron-oxide-rich red earth soils. *J. Colloid Interface Sci.* **2013**, *406*, 217–224. [[CrossRef](#)] [[PubMed](#)]
21. Lu, H.; Zhu, Z.; Zhang, H.; Zhu, J.; Qiu, Y. Simultaneous removal of arsenate and antimonate in simulated and practical water samples by adsorption onto Zn/Fe layered double hydroxide. *Chem. Eng. J.* **2015**, *276*, 365–375. [[CrossRef](#)]
22. Qi, P.; Pichler, T. Sequential and simultaneous adsorption of Sb(III) and Sb(V) on ferrihydrite: Implications for oxidation and competition. *Chemosphere* **2016**, *145*, 55–60. [[CrossRef](#)] [[PubMed](#)]
23. Leuz, A.K.; Mönch, H.; Johnson, C.A. Sorption of Sb(III) and Sb(V) to goethite: Influence on Sb(III) oxidation and mobilization. *Environ. Sci. Technol.* **2006**, *40*, 7277–7282. [[CrossRef](#)] [[PubMed](#)]
24. Belzile, N.; Chen, Y.W.; Wang, Z. Oxidation of antimony(III) by amorphous iron and Manganese oxyhydroxides. *Chem. Geol.* **2001**, *174*, 379–387. [[CrossRef](#)]
25. Xu, W.; Wang, H.; Liu, R.; Zhao, X.; Qu, J. The mechanism of antimony(III) removal and its reactions on the surfaces of Fe-Mn Binary Oxide. *J. Colloid Interface Sci.* **2011**, *363*, 320–326. [[CrossRef](#)] [[PubMed](#)]
26. Liu, R.; Liu, F.; Hu, C.; He, Z.; Liu, H.; Qu, J. Simultaneous removal of Cd(II) and Sb(V) by Fe-Mn binary oxide: Positive effects of Cd(II) on Sb(V) adsorption. *J. Hazard. Mater.* **2015**, *300*, 847–854. [[CrossRef](#)] [[PubMed](#)]
27. Sazakli, E.; Zouvelou, S.V.; Kalavrouziotis, I.; Leotsinidis, M. Arsenic and antimony removal from drinking water by adsorption on granular ferric oxide. *Water Sci. Technol.* **2015**, *71*, 622–629. [[CrossRef](#)] [[PubMed](#)]
28. Ilavský, J.; Barloková, D.; Munka, K. Antimony Removal from Water by Adsorption to Iron-Based Sorption Materials. *Water Air Soil Pollut.* **2015**, *226*, 2238. [[CrossRef](#)]
29. Kolbe, F.; Weiss, H.; Morgenstern, P.; Wennrich, R.; Lorenz, W.; Schurk, K.; Stanjek, H.; Daus, B. Sorption of aqueous antimony and arsenic species onto akaganeite. *J. Colloid Interface Sci.* **2011**, *357*, 460–465. [[CrossRef](#)]
30. Tresintsi, S.; Simeonidis, K.; Zouboulis, A.; Mitrakas, M. Comparative study of As(V) removal by ferric coagulation and oxy-hydroxides adsorption: Laboratory and full-scale case studies. *Desalin. Water Treat.* **2013**, *51*, 2872–2880. [[CrossRef](#)]
31. Tresintsi, S.; Simeonidis, K.; Vourlias, G.; Stavropoulos, G.; Mitrakas, M. Kilogram-scale synthesis of iron oxy-hydroxides with improved arsenic removal capacity: Study of Fe(II) oxidation–precipitation parameters. *Water Res.* **2012**, *46*, 5255–5267. [[CrossRef](#)] [[PubMed](#)]
32. European Committee for Standardization. 2002. EN 12457-2: Characterization of Waste—Leaching—Compliance Test for Leaching of Granular Waste Materials and Sludges—Part 2: One Stage Batch Test at Liquid to Solid Ratio of 10 L/kg for Materials with Particle Size below 4 mm (without or with Size Reduction). European Standard; European Committee for Standardization: Brussels, Belgium, 2002.
33. Tripathy, S.S.; Raichur, A.M. Enhanced adsorption of activated alumina by impregnation with alum for removal of As(V) from water. *Chem. Eng. J.* **2008**, *138*, 179–186. [[CrossRef](#)]
34. Cumming, L.J.; Chen, A.S.C.; Wang, L. *Arsenic and Antimony Removal from Drinking Water by Adsorption Media, US EPA Demonstration Project at South Truckee Meadows General Improvement District (STMGID)*; NV, Final Performance Evaluation Report; EPA/600/R-09/016; US Environmental Protection Agency: Washington, DC, USA, February 2009.

